Arab J Sci Eng (2016) 41:1723–1733
DOI 10.1007/s13369-015-1942-0

RESEARCH ARTICLE - MECHANICAL ENGINEERING

Optimization of Biofuel Blends and Compression Ratio of a Diesel Engine Fueled with *Calophyllum inophyllum* Oil Methyl Ester

G. Antony Miraculas[1] · **N. Bose**[2] · **R. Edwin Raj**[1]

Received: 24 June 2015 / Accepted: 19 October 2015 / Published online: 4 November 2015

Abstract The twin crises in depletion of fossil fuels and environmental degradation have motivated researches to consolidate the use of biofuels for internal combustion engine applications. In the present study, the performance and emission characteristic of *Calophyllum inophyllum* oil-based methyl ester and its diesel blends are analyzed at various compression ratios. Comprehensive optimization by considering the performance parameter along with emission characteristic is rather involved and is done carefully with designed set of experiments and analyzed statistically using design expert software. Higher compression ratio (CR) induces high cylinder temperature which enhances vaporization and thereby better performance only to a certain extent, that is, up to a CR of 19. However, due to high operating temperature, the oxides of nitrogen emission increase with CR and also for high biofuel blends, but better combustion phenomenon at these conditions reduces the emissions of carbon monoxide and unburned hydrocarbon. The designed empirical statistical model for optimum performance with lower emission is found to be B30 (30 % biofuel) at a CR of 19, which is then tested and validated.

✉ R. Edwin Raj
redwinraj@gmail.com

G. Antony Miraculas
miraculas@gmail.com

N. Bose
bosevnr@gmail.com

1 St. Xavier's Catholic College of Engineering, Chunkankadai, Nagercoil 629003, India

2 Mepco Schlenk Engineering College, Sivakasi 626005, India

Keywords Biofuel · Compression ratio · Blends · Emission

1 Introduction

The ever-increasing energy demand due to increasing vehicle population depletes fossil fuel and increases its cost. These critical aspects have made researchers to find viable, sustainable and environmental friendly alternate fuel. In this line, biodiesel extraction from nonedible vegetable oil sources can definitely augment to meet the rapidly growing energy needs of the world, especially in countries where there are less fossil fuel resources. Biodiesel is monoalkyl esters of long-chain fatty acids derived from lipid feed stocks such as vegetable oils and animal fats. Countries like India cannot afford to produce biodiesel from edible oils, because of its food processing needs. Biodiesel extraction from nonedible seeds such as rubber seed [1], cotton seed [2], polanga [3], Eruca Sativa Gars [4], rape seed [5], neem [6], mahua [7], Pongamia pinnata [8] and jatropha curcas [9] were explored, which needs to be sustained and consolidated for mass production.

Vegetable oil has comparable and competent physical properties of diesel such as cetane number, energy density and heat of combustion. However, their viscosity is higher than that of diesel, which hinders effective management of fuel pumping, atomization, vaporization and combustion. Transesterification is one of the methods extensively and effectively used to reduce its viscosity by breaking the long-chain fatty acids into monoesters [1].

The performance of biodiesel and its blends with diesel on internal combustion (IC) engines have shown varied inferred deduction in comparison with that of diesel. Some researchers have got better performance at lower percentage of biodiesel blends and have attributed it to the oxygenated nature of fatty acid methyl ester (FAME). Moreover, the effect of increased

viscosity is insignificance at lower concentration of biodiesel [10,11]. Few researches have reported an increase in brake thermal efficiency (BTE) for pure biodiesel than that of its blend and diesel, due to less friction because of better lubricity, in addition to the presence of inherent oxygen in biofuel [12]. However, reduction in BTE for biodiesel and its blends are also being reported [13–15]. Break specific fuel consumption (BSFC) is defined as the amount of fuel required for developing unit power, which has to be minimum for optimum performance. Generally, BSFC is higher for biodiesel and its blends when compared with that of diesel due to its lower calorific value and higher density [11,16–19]. Sahoo et al have reported insignificant difference in comparison with diesel [3]; however, some reports have even shown lower BSFC for 20 and 40 % biodiesel blends [20].

Biodiesel being an oxygenated fuel facilitates complete combustion, and its high cetane number reduces the ignition delay, which enables the process of combustion within the stipulated period. These things will complement each other for complete combustion, thereby reducing CO emission [11,18]. However, increase in CO emission for pure jatropha biodiesel is also reported owing to high viscosity [21]. Biodiesel is a sulfur-free fuel; therefore, sulfate emissions are less [22,23]. Several researchers have reported low hydrocarbon (HC) emission for biodiesel in comparison with diesel, mainly due to the oxygenated nature of biodiesel [3,15–17,21,24]. Few have also reported an increase in HC emission due to its low volatility and high viscosity, which leads to poor atomization and vaporization [25].

NOx are formed due to the oxidation of nitrogen at very high temperatures. Again the literatures are divided in its finding on NOx emission from IC engines. 10–15 % higher NOx emission for biodiesel is reported and attributed it to the oxygenated nature of biofuel [11,18,21,26,27]. Few others have reported no difference or insignificant difference in NOx emission [23,25]. Also, some have even reported reduction in NOx emission [19,28–30]. Sahoo et al. [3] have found that the NOx emission for biodiesel blends is greater than that of diesel, whereas pure biodiesel emits 4 % lesser NOx emission.

In spite of research in biodiesel extraction and performance analysis in IC engines, comprehensive characterization of the same is rather sparse, but essential for consolidating the continuing research to commercialize it in the market. In this work, nonedible *Calophyllum inophyllum* oil-based biodiesel is extracted under optimized process conditions and tested in IC engine. Robust statistical optimization tool design of experiment is employed to optimize the compression ratio (CR) and biodiesel–diesel blend for better performance in a single-cylinder compression ignition engine. Emission parameters such as CO, HC and NOx are also determined to ascertain the pollution limits during test conditions.

2 Extraction of Biofuel and Testing of Its Property

The nonedible oil extracted from the seeds of *C. inophyllum* plant had high fatty acid content (48 mg KOH/g) which demands a two-stage esterification process for its conversion into biodiesel. The effectiveness of esterification process is in turn dependent on various input parameters; multivariant design of experiments is employed to optimize the major influencing process parameters. Accordingly, methanol-to-oil ratio, catalytic concentration, reaction temperature and the duration of reaction are considered as input parameters for both acid and alkaline esterification stages. After optimizing the parameters for effective reduction in acid value in the first stage, the second-stage input variables are optimized for maximizing the methyl ester yield. Under the optimized condition, enough quantity of biofuel is extracted for testing the same in engine after fuel characterization. Details of extraction process and optimization are published by the same authors elsewhere [31].

Standard test procedures are followed for the determination of extracted *C. inophyllum* oil methyl ester properties. The viscosity is noted at 40 °C under atmospheric pressure using BROOKFIELD LV-DV-II+ Pro viscometer, Middleboro, USA. The viscosity of raw *C. inophyllum* seed oil is reduced from 45.8 to 4.2 mm^2/s by two-stage esterification process to keep it within the ASTM D6751-02 standard for biodiesel. The extracted biodiesel is tested for its chemical composition using gas chromatograph, GC 200-3A-CIC. The major fatty acid components in esters are palmitic acid, stearic acid, oleic acid and linoleic acid (Fig. 1). Oleic acid oils are resistance to oxidation; therefore, it can be used as an alternative fuel for diesel engines. The flash point and

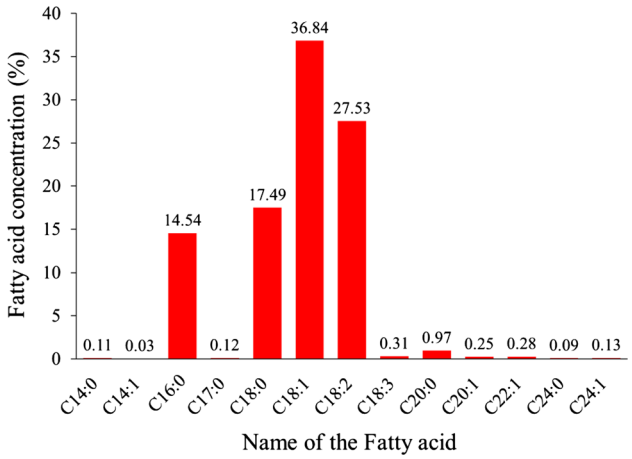

Fig. 1 Fatty acid profile for methyl esters of *C. inophyllum* oil by GC analysis. C14:0—myristic acid; C14:1— myristoleic acid; C16:0—palmitic acid; C17:0—heptadecaenoic acid; C18:0—stearic acid; C18:1—oleic acid; C18:2—linoleic acid; C18:3—linolenic acid; C20:0—arachidic acid; C20:1—eicosenoic acid; C22:1—docosenoic acid; C24:0—lignoceric acid; C24:1—nervonic acid

Table 1 Properties of *C. inophyllum* oil biodiesel in comparison with diesel

Properties	Diesel	Biodiesel standard ASTM D6751-02	*Calophyllum inophyllum* oil methyl ester
Kinematic viscosity @ 40 °C (mm^2/s)	3.18	1.9–6.0	4.2
Flash point (°C)	68	130	110
Specific gravity	0.839	0.87–0.90	0.885
Calorific value (kJ/kg)	43600	–	40800
Pour point (°C)	−20	−1.5 to 10	3

fire point of biodiesel are determined by using the Pensky–Martens closed cup apparatus. The energy content of the fuel is measured using standard 6772 calorimetric thermometer as 40,800 kJ/kg, which is very close to that of diesel to ensure satisfactory performance with the existing diesel engine [31]. The properties of tested *C. inophyllum* seed-based biofuel are listed along with diesel and ASTM standard biodiesel in Table 1.

3 Experimental Setup

Tests are conducted in a single-cylinder, four-stroke, water-cooled engine with facilities to vary the CR by moving the cylinder head. The engine is loaded with an eddy current dynamometer. Data such as crank angle, cylinder and injection pressure, air flow rate, fuel flow rate and temperatures are simultaneously acquired using a data acquisition system and recorded in a computer. The major engine specifications are provided in Table 2.

Exhaust gas analysis is done by sampling directly from the exhaust line without affecting the back-pressure with a specially designed arrangement by the multigas analyzer. The concentrations of CO, HC and NOx (specification in Table 3) in the engine exhaust are recorded continuously, and a separate smoke meter is used to detect and measure the quantity of smoke emitted from the engine.

Table 2 Specification of the given test engine

Description	Specification
No. of cylinder	One
Type of cooling	Water cooling
Cycle	Four stroke
Bore	87.5 mm
Stroke	110 mm
Displacement volume	661 cc
Piston	Hemispherical
Compression ratio	16–22
Rated power	5 kW @ 1600 RPM
Injection timing	23 °BTDC
Nozzle opening pressure	210 bar
Loading	Eddy current dynamometer
Temperature sensor	Type K—chromel

Table 3 Specification of the exhaust gas analyzer

Parameter	Resolution	Accuracy	Range
CO	0.001 %	±0.02 %	0–9.99 %
HC	1 ppm	±10 ppm	0–5000 ppm
NOx	1 ppm	±10 ppm	0–5000 ppm

4 Results and Discussion

Various studies have shown that the engine performance depends on both biodiesel–diesel blend and the CR of the engine. Test are performed with *C. inophyllum* seed-based biodiesel and its blend in the engine using the designed test conditions to optimize the CR and fuel blend for better performance. The major engine performance parameters such as BTE and BSFC and emission characteristics such as CO, HC, NOx and smoke are analyzed.

4.1 Brake Thermal Efficiency

The CR of the engine is varied from 16 to 22 in steps of two, and the biodiesel is blended with diesel in percentage as 0, 20, 40, 60 and 100 %. A series of experiments are conducted in the VCR engine to evaluate the relevance of CR and biodiesel blend in reducing the emission and BSFC, thereby maximizing the BTE. The outcomes are analyzed by using analysis of variance, and the results are shown in Table 4. Before drawing any inference, the model has to be validated satisfactorily. The model p value is <0.0001 which indicates that the model terms considered are significant, with a F value of 57.78. There is significant interactive effect (p value of AB is <0.05) between CR (A) and the amount of biodiesel in the blend (B) in the process which cannot be inferred by simple experiments and was taken care by the surface response model (Fig. 2). The "Predicted R-Squared" value of 0.8795 is in reasonable agreement with the "Adjusted R-Squared" of 0.9642. "Adeq Precision" measures the signal-to-noise ratio,

Table 4 ANOVA for BTE model

Source	Sum of squares	*df*	Mean square	*F* value	*p* value prob > *F*
Model	192.86	9	21.4	57.8	<0.0001
A–A	8.53	1	8.5	23.0	0.0007
B–B	38.26	1	38.3	103.2	<0.0001
AB	4.95	1	4.9	13.3	0.0044
A^2	23.05	1	23.1	62.2	<0.0001
B^2	5.00	1	5.0	13.5	0.0043
Residual	3.71	10	0.4		
Cor total	196.57	19			

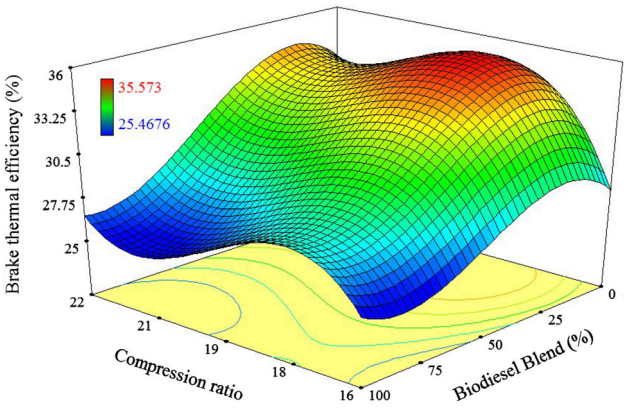

Fig. 2 RSM plot for brake thermal efficiency

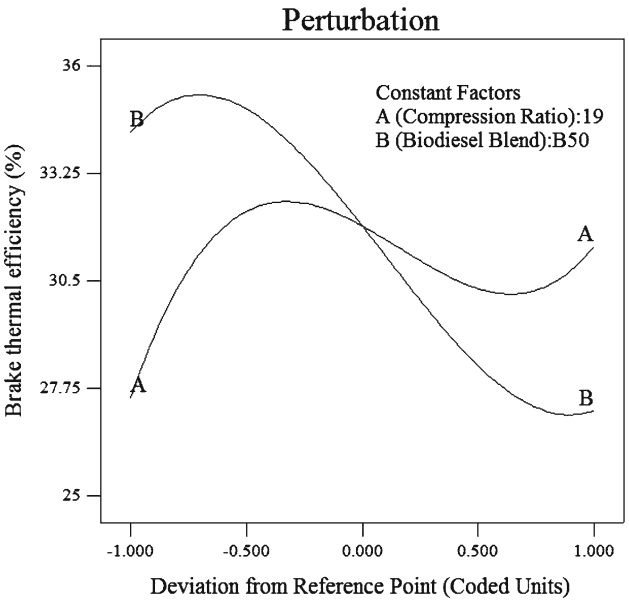

Fig. 3 Perturbation plot for brake thermal efficiency

and a value >4 is desirable, and for this model, it is 22.92, which indicates that the signals are adequate enough. The analysis of variance signifies that the model can be used to navigate the design space. The 3D plot shows the variation of BTE with the CR and fuel blends (Fig. 2). It is pragmatic that BTE decreases with biodiesel blend and, however, there is a slight increase in BTE for B20. The average BTE of B20 is about 4.1 % higher than that of pure diesel. The presence of oxygen might have enhanced combustion, and the negative effect of increased viscosity might not have activated. The average BTE of pure biodiesel at full load for all compression ratios is 15.6 % lower than that of diesel. The maximum BTE of diesel is 34.6 %, while in case of 20, 40, 60 and 100 % biodiesel blend, the BTE is 35.6, 34.4, 30.8 and 29.4 %, respectively.

The perturbation plot (Fig. 3) compares the influence of various factors at a specific point in the design space. A positive slope for the factor *A*, the CR, indicates that the BTE increases with increase in CR, and at higher CR, the curve is almost flat, which indicates that it has no significance. The negative slope for blend implies that the BTE decreases with increase in biodiesel blend, whereas a fairly flat line at the beginning indicates that at lower blends, there is only a slight increase in brake thermal efficiency. A three-dimensional response plot is drawn with CR and blend as axis in relation to BTE. The optimum parameter for maximizing the BTE is obtained at a CR of 19 and with a biodiesel blend of 15 %.

4.2 Brake Specific Fuel Consumption

Experimental results at full load reveal that as the CR of the engine increases, BSFC decreases up to the CR of 19; afterward, its significance reduces and even reverses at higher CR. The analysis of variance result is shown in Table 5. Since the response is nonlinear, the response surface cubic model is selected. The model *F* value of 43.83 and the *p* value of <0.001 signify the significance of the model for deriving inference. The "Predicted R-Squared" of 0.8832 is in reasonable agreement with the "Adjusted R-Squared" of 0.9530. The "Adeq Precision" value of the present model is 23.28 which indicates adequate signal, which allows the model to be navigated in the designed space.

The perturbation plot compares the influence of various factors at a specific point in the design space (Fig. 4). A fairly

Table 5 ANOVA for BSFC model

Source	Sum of squares	*df*	Mean square	*F* value	*p* value prob > F
Model	0.018	9	1.99E−03	43.83	<0.0001
A–A	2.32E−05	1	2.32E−05	0.51	0.4909
B–B	6.20E−03	1	6.20E−03	136.74	<0.0001
AB	9.17E−07	1	9.17E−07	0.02	0.8898
A^2	2.74E−03	1	2.74E−03	60.47	<0.0001
B^2	1.22E−03	1	1.22E−03	26.82	0.0004
Residual	4.54E−04	10	4.54E−05		
Cor total	0.018	19			

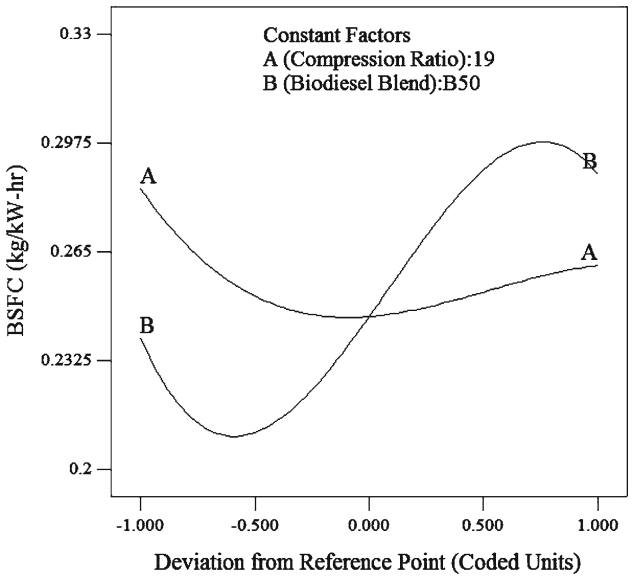

Fig. 4 Perturbation plot for brake specific fuel consumption

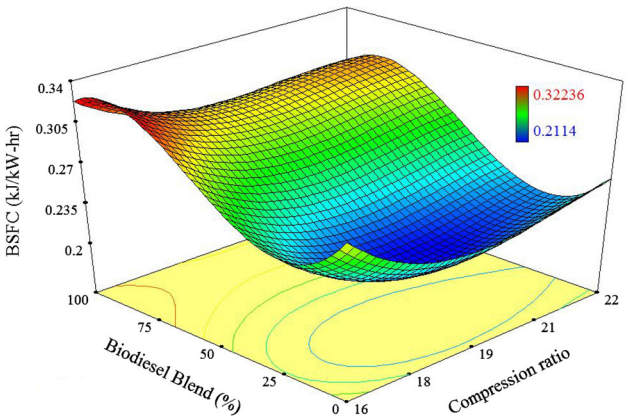

Fig. 5 RSM plot for BSFC

negative slope for the factor *A*, the CR, indicates that the BSFC decreases with increase in CR. The BSFC of diesel and biodiesel declines on an average by 9.3 and 10.5 %, respectively, as the CR is augmented from 16 to 18. The equivalent value for further increase in CR from 18 to 20 is only 0.2 and 4.1 %, respectively. This shows that the benefits of increased CR are more for biodiesel than diesel, which might be due to the low volatility and increased viscosity of biodiesel. For factor *B* (biodiesel blend), the curve has an initial valley-like portion and it steeps further to bend again at higher CRs, which implies that the BSFC increases with increase in biodiesel concentration. This may be due to the lower calorific value of biodiesel and the negative effect of higher CR. Figure 5 is a surface response model that shows the influence of CR and biodiesel blend on BSFC at full load. It can be observed from the contour of Fig. 4 that BSFC is lower in the region of CR19, where the biodiesel blend is around 20 % which seems to be the optimum range for better performance.

4.3 Carbon Monoxide Emission

Partially burned fuel causing CO emission is hazardous to human health, which needs to be minimized through appropriate technology. The CO emissions for each experiment are recorded carefully by varying the CR and fuel blends. Empirical model is generated from the experimental data by mapping the outcome for the given input. The analysis of variance is done to ensure the adequacy of the model, and the results are shown in Table 6. The model *p* value of <0.0001 (*F* value of 160.9) indicates that the model terms considered are significant. The *F* value for CR and biodiesel blend models is 337.47 and 368.07, respectively, which infers that the influence of these factors on CO emission is significant. The "Predicted R-Squared" value of 0.9614 is in reasonable agreement with the "Adjusted R-Squared" value of 0.9768. The analysis of variance signifies that the model can be used to navigate the design space. Figure 6 shows the three-dimensional response plot with CR and biodiesel blend as axis in relation to CO emission.

The perturbation plot (Fig. 7) shows the influence of CR and fuel blend on CO emission in the design space. The negative slope for the factor *A*, the CR, indicates that the CO emission decreases with increase in CR and saturates at higher CRs. The average reduction in CO emission for B100

Table 6 ANOVA for CO emission model

Source	Sum of squares	*df*	Mean square	*F* value	*p* value prob > F
Model	0.013	5	2.541E−003	160.90	<0.0001
A–A	5.328E−003	1	5.328E−003	337.47	<0.0001
B–B	5.812E−003	1	5.812E−003	368.07	<0.0001
AB	7.420E−005	1	7.420E−005	4.70	0.0479
A^2	1.037E−003	1	1.037E−003	65.66	<0.0001
B^2	1.429E−004	1	1.429E−004	9.05	0.0094
Residual	2.211E−004	14	1.579E−005		
Cor total	0.013	19			

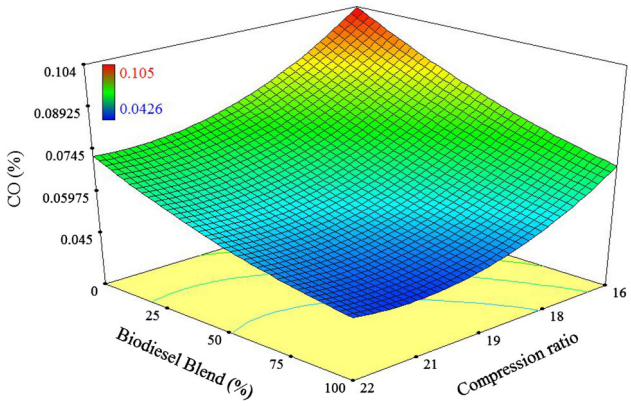

Fig. 6 RSM plot for carbon monoxide emissions

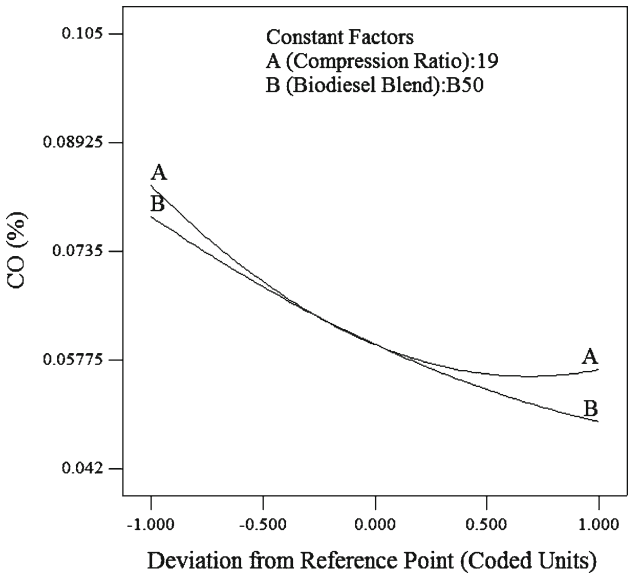

Fig. 7 Perturbation plot for carbon monoxide emission

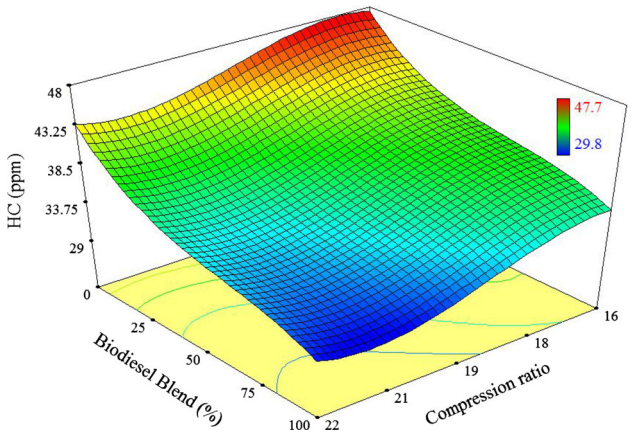

Fig. 8 RSM plot for unburned HC emission

fuel compared with diesel for CR of 16, 18, 20 and 22 is 22.68, 34.86, 42.74 and 33.33 %, respectively. At lower CR, the reduction in CO emission is slightly lesser because of reduced heat generation due to compression which in turn delays the start of ignition. As the CR increases, the temperature of air inside the engine cylinder also increases, thereby reducing the ignition delay, which leads to complete burning of fuel. Similarly negative slope is obtained for biodiesel blend also, which implies that the CO value decreases with increase in biodiesel concentration and it is lowest for pure biodiesel due to the presence of oxygen in the fuel itself which enhances combustion.

4.4 Hydrocarbon Emission

Unburned fuel escapes along with the exhaust gas as HC emissions. Figure 8 shows the response surface plot for the variations of unburned HC emission with respect to the CR and biodiesel blends. The analysis of variance is done to validate the model for deriving inference (Table 7). The model *F* value of 88.55 implies that the model is significant. The "Predicted R-Squared" value of 0.9364 is close to that of the "Adjusted R-Squared" value of 0.9765. The signal-to-noise ratio of 32.563 indicates adequacy of signal, which allows the model to be navigated in the designed space.

The sharp negative slope in the perturbation chart for the factor *B*, biodiesel blend indicates its significant influence on the emission of HC (Fig. 9). As the percentage of biodiesel content is increased in the fuel, the emission of

Table 7 ANOVA for HC emission model

Source	Sum of squares	*df*	Mean square	*F* value	*p* value prob > F
Model	480.01	9	5.33E+01	88.55	<0.0001
A–A	2.56E+01	1	2.56E+01	42.5	<0.0001
B–B	1.06E+01	1	1.06E+01	17.52	0.0019
AB	8.10E−01	1	8.10E−01	1.35	0.2725
A^2	3.64E+00	1	3.64E+00	6.05	0.0337
B^2	1.78E+01	1	1.78E+01	29.48	0.0003
Residual	6.02E+00	10	6.00E−01		
Cor total	486.04	19			

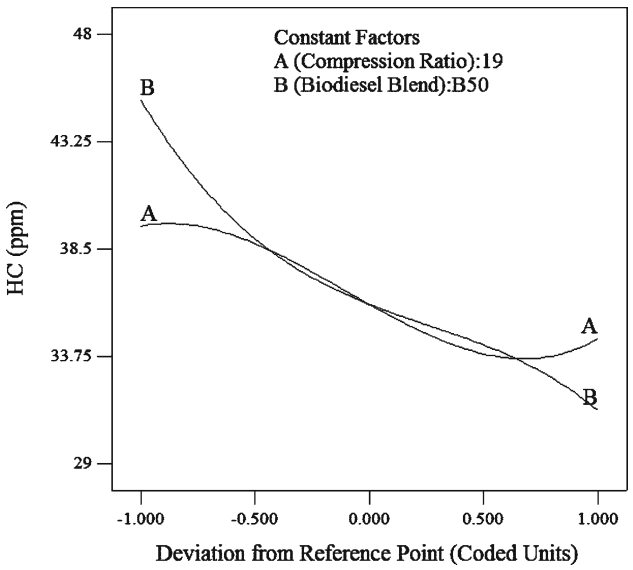

Fig. 9 Perturbation plot for unburned HC emission

HC decreases and it is minimum for B100. The inbuilt oxygen in the biodiesel enhances complete combustion of fuel which ensures lesser emission of unburned HC. Similarly, as the CR increases, the emission of HC also decreases and reaches a saturation value around a CR of 19. The reduction in HC emission when compared with diesel for CR 16 and 18 is almost identical and is around 26–28 %. However, at CR 20, a maximum reduction in HC emission of about 34 % is observed for B100 fuel when compared with diesel. Conversely, the HC reduction is lesser at high CR when compared with diesel due to the dilution of air by residual gases, which hinders the combustion. The operating temperature is higher for higher CR, and it ensures better vaporization, which leads to efficient combustion, and reduced HC emission for biodiesel.

4.5 Oxides of Nitrogen Emission

NOx emission is one of the precarious emissions from the diesel engine due to high in-cylinder temperature where nitrogen oxidize to form NOx. The analysis of variance is done to test the significance of the model, and the results are tabulated in Table 8. The model *p* value is <0.0001 with a corresponding *F* value of 182.77, which indicates that the model terms considered are significant. The most significant model term is the CR (factor *A*) with an *F* value of 851.43, which indicates that the NOx emission increases significantly with CR due to higher combustion temperature. The "Predicted R-Squared" value of 0.9723 is in reasonable agreement with the "Adjusted R-Squared" of 0.9795, and the signal-to-noise ratio is 38.47, which indicates that the signals are adequate enough.

4.6 Smoke Emission

The perturbation plot (Fig. 10) shows a sharp positive slope for the factor *A*, the CR, which indicates the direct connection

Table 8 ANOVA for NOx emission model

Source	Sum of squares	*df*	Mean square	*F* value	*p* value prob > F
Model	4.859E+005	5	97177.06	182.77	<0.0001
A–A	4.527E+005	1	4.527E+005	851.43	<0.0001
B–B	13351.39	1	13351.39	25.11	0.0002
AB	2309.45	1	2309.45	4.34	0.0560
A^2	6919.20	1	6919.20	13.01	0.0029
B^2	9309.60	1	9309.60	17.51	0.0009
Residual	7443.69	14	531.69		
Cor total	4.933E+005	19			

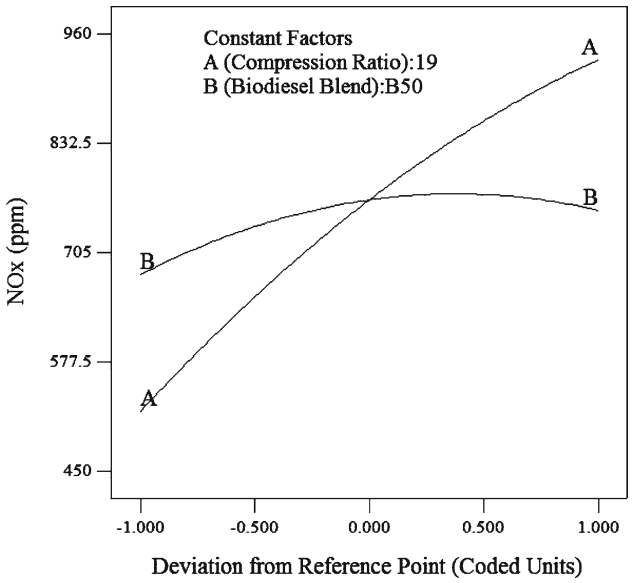

Fig. 10 Perturbation plot for oxides of nitrogen emission

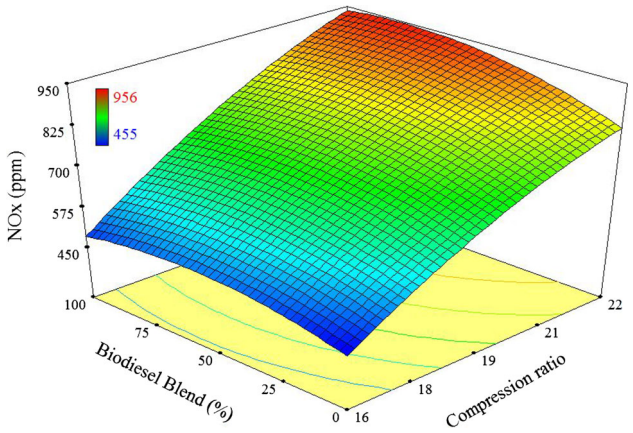

Fig. 11 RSM plot for oxides of nitrogen emission

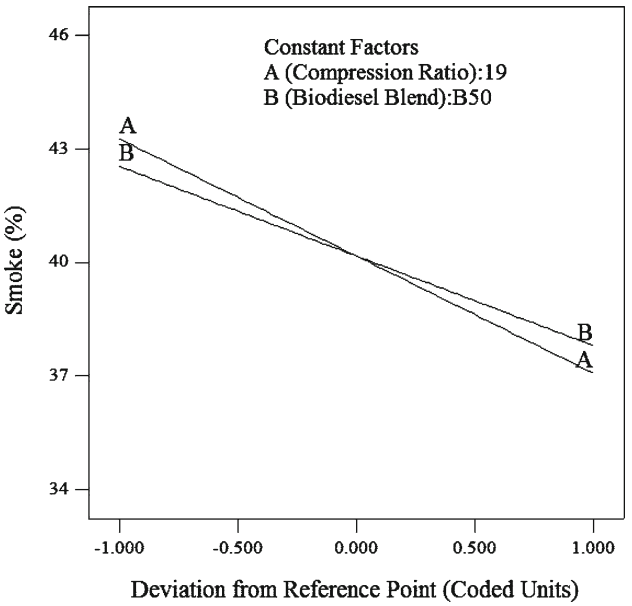

Fig. 12 Perturbation plot for smoke emission

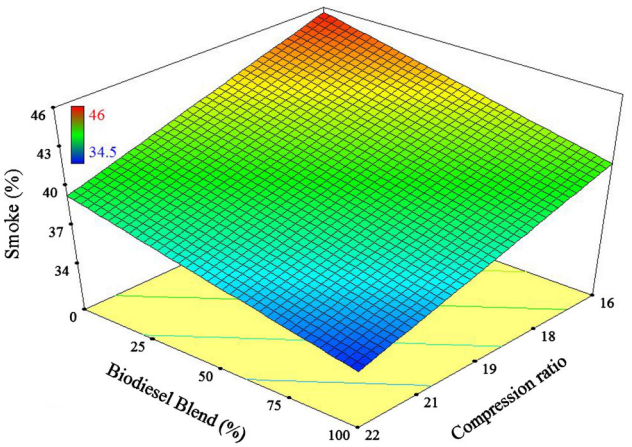

Fig. 13 RSM plot for smoke emission

for NOx emission with increase in CR. The NOx emission is observed as 460, 609, 760 and 825 ppm at CR 16, 18, 20 and 22, respectively, for diesel fuel. It is also observed that the NOx emission for B100 increases by 6.9, 9.6, 10.1 and 14.2 % at CR of 16, 18, 20 and 22, respectively, in comparison with diesel fuel. The lower CR reduces the in-cylinder temperature, which in turn reduces the flame temperature during combustion to suppress the NOx emission. The gradual positive slope for biodiesel blend (factor *B*) shows that it has little influence on deciding the NOx emission. Figure 11 shows the three-dimensional response surface model, where the variation of NOx with the compression ratios and biodiesel blends is depicted. It can be observed that the NOx value increases with the CR and with the quantity of biodiesel blending. The

Table 9 ANOVA for smoke emission model

Source	Sum of squares	*df*	Mean square	*F* value	*p* value prob > F
Model	159.23	2	79.62	54.71	<0.0001
A–A	106.30	1	106.30	73.05	<0.0001
B–B	52.94	1	52.94	36.38	<0.0001
Residual	24.74	17	1.46		
Cor total	183.97	19			

Table 10 The optimum projected parameters and the predicted performance and emission using DOE

A (CR)	B (Blend)	BTE (%)	BSFC (kg/KW-h)	CO (%)	HC (ppm)	NOx (ppm)	Smoke (%)
19	28.68	34.59	0.213	0.067	38.3	745.3	41.12

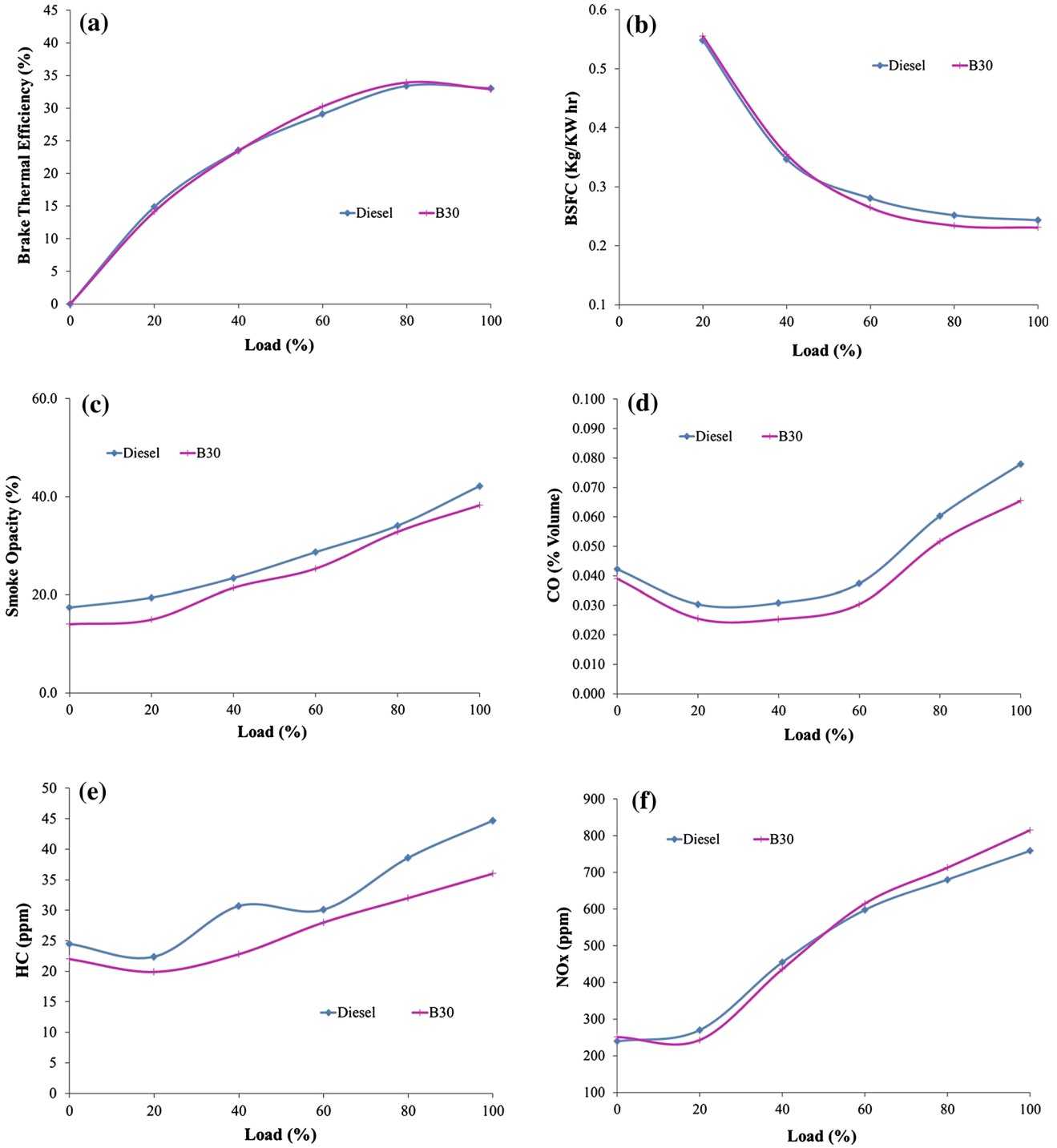

Fig. 14 Engine performance and emission at optimum predicted compression ratio (CR:19) and blend (B30) at various loads. **a** Variation of BTE with engine load. **b** Variation of BSFC with engine load. **c** Variation of smoke opacity with engine load. **d** Variation of CO emission with engine load. **e** Variation of HC emission with engine load. **f** Variation of NOx emission with engine load

operating temperature for biodiesel is always higher than that of diesel due to the presence of inbuilt oxygen, which promotes early combustion and thereby increases the retention time of combustion gases.

The smoke opacity is also measured while conducting experiments by varying the CR and biodiesel blends. The ANOVA results are tabulated in Table 9 which shows that the model p value is <0.0001 with a corresponding F value of 54 indicating significance of the model. The "Predicted R-Squared" value of 0.8123 is in reasonable agreement with the "Adjusted R-Squared" value of 0.8497, and the signal-to-noise ratio of 23.36 indicates the adequacy of signal to navigate the design space. The perturbation plot (Fig. 12) shows a sharp slope for factor A (CR) and B (biodiesel blend), indicating that the smoke emissions are sensitive to these factors. Figure 13 shows that the smoke emissions at higher CR are lesser than at lower CR, since at higher CR the operating pressure and temperature increase, which eventually increases the combustion efficiency. It is also observed that for a given CR, the smoke emissions for biodiesel and its blends are always lesser than that of diesel and it reduces with increase in biodiesel blends. This phenomenon is attributed to the presence of oxygen in the molecules of biodiesel.

4.7 Optimization and Validation

Design of experiments is used to find the optimum CR and the biodiesel blend to achieve higher BTE and lower BSFC and to reduce emission level of smoke, NOx, CO, HC, etc. Table 10 shows the projected CR and blend with lower emissions and higher efficiency using the empirical model.

The empirical model predication values are validated by experimental work using the given input parameters and found that the predicted values are close to that of the experimental value (Fig. 14a–e). Figure 14b shows the variation of BSFC with respect to load. It can be noted that the BSFC of B30 at higher loads is lesser than that of diesel. This may be due to the presence of dissolved oxygen in the blend that enables complete combustion at higher loads. Since only 30 % of biodiesel is blended with diesel, the negative effects of higher viscosity of biodiesel are not prominent. Figure 14c–e shows that the smoke, HC and CO emissions of B30 decrease significantly and are found to be analogs with those of the predicted value. Figure 14f shows that the oxides of nitrogen emissions for B30 at higher loads are higher than those of diesel, which may be due to the inherent presence of oxygen molecules along with the fuel.

5 Conclusion

Underutilized, nonedible *C. inophyllum* oil is used to extract biodiesel through optimized two-stage esterification process. The fuel properties are tested with standard test procedures and blended with diesel in proportion of 20, 40, 60 and 100 %. They are then tested in engine to optimize the CR and biodiesel blending, based on engine performance and emission. Optimization is done by conducting designed experiments to develop empirical statistical model using design experts software. The model is then validated by experiments before deriving objective inferences. It is observed that BTE increases with CR up to 19 for all blends and is especially maximum for the fuel blend of 20 % biodiesel. Considering the combined objective to maximize brake thermal efficiency and to reduce emission, B30 blend and CR19 are predicted by the empirical model, which is validated experimentally and found to be in close range.

References

1. Melvin Jose, D.F.; Edwin Raj, R.; Durga Prasad, D.; Robert Kennedy, Z.; Mohammed Ibrahim, A.: A multi-variant approach to optimize process parameters for biodiesel extraction from rubber seed oil. Appl. Energy **88**, 2056–2063 (2011)
2. Royon, D.; Daz, M.; Ellenrieder, G.; Locatelli, S.: Enzymatic production of biodiesel from cotton seed oil using t-butanol as a solvent. Bioresour. Technol. **98**, 648–653 (2007)
3. Sahoo, P.K.; Das, L.M.; Babu, M.K.G.; Naik, S.N.: Biodiesel development from high acid value polanga seed oil and performance evaluation in a CI engine. Fuel **86**, 448–454 (2007)
4. Li, S.; Wang, Y.; Dong, S.; Chen, Y.; Cao, F.; Chai, F.; Wang, X.: Biodiesel production from Eruca Sativa Gars vegetable oil and motor, emissions properties. Renew. Energy **34**(7), 1871–1876 (2009)
5. Qi, D.H.; Lee, C.F.; Jia, C.C.; Wang, P.P.; Wub, S.T.: Experimental investigations of combustion and emission characteristics of rapeseed oil–diesel blends in a two cylinder agricultural diesel engine. Energy Convers. Manag. **77**, 227–232 (2014)
6. Dhar, A.; Kevin, R.; Agarwal, A.K.: Production of biodiesel from high-FFA neem oil and its performance, emission and combustion characterization in a single cylinder DICI engine. Fuel Process. Technol. **97**, 118–129 (2012)
7. Ghadge, S.V.; Raheman, H.: Process optimization for biodiesel production from mahua (*Madhuca indica*) oil using response surface methodology. Bioresour. Technol. **97**, 379–384 (2006)
8. Naik, M.; Meher, L.C.; Naik, S.N.; Das, L.M.: Production of biodiesel from high free fatty acid Karanja (*Pongamia pinnata*) oil. Biomass Bioenergy **32**, 354–357 (2008)
9. Koberg, M.; Gedanken, A.: Direct transesterification of castor and Jatropha seeds for FAME production by microwave and ultrasound radiation using a SrO catalyst. BioEnergy Res. **5**, 958–968 (2012)
10. Ramadhas, A.S.; Jayaraj, S.; Muraleedharan, C.: Characterization and effect of using rubber seed oil as fuel in the compression ignition engines. Renew. Energy **30**, 795–803 (2005)
11. Buyukkaya, E.: Effects of biodiesel on a DI diesel engine performance, emission and combustion characteristics. Fuel **89**, 3099–3105 (2010)
12. Murillo, S.; Mı'guez, J.L.; Porteiro, J.; Granada, E.; Mora'n, J.C.: Performance and exhaust emissions in the use of biodiesel in outboard diesel engines. Fuel **86**, 1765–1771 (2007)
13. Desantes, J.M.; Arregle, J.; Ruiz, S.; Delage, A.: Characterization of the Injection–Combustion Process in a D.I. Diesel Engine Running with Rape Oil Methyl Ester, SAE 1999-01-1497, pp. 984–991 (1997)

14. Hamasaki, K.; Tajima, H.; Takasaki, K.; Satohira, K.; Enomoto, M.; Egawa, H.: Utilization of waste vegetable oil methyl ester for diesel fuel, SAE 2001-01-2021, pp. 1499–1504 (2001)
15. Jindal, S.; Nandwana, B.P.; Rathore, N.S.; Vashistha, V.: Experimental investigation of the effect of compression ratio and injection pressure in a direct injection diesel engine running on jatropha methyl ester. Appl. Therm. Eng. **30**, 442–448 (2010)
16. Dorado, M.P.; Ballesteros, E.; Arnal, J.M.; Gomez, J.; Lopez, F.J.: Exhaust emissions from a diesel engine fueled with transesterified waste olive oil. Fuel **82**, 1311–1315 (2003)
17. Rao, G.L.N.; Sampath, S.; Rajagopal, K.: Experimental studies on the combustion and emission characteristics of a diesel engine fuelled with used cooking oil methyl ester and its diesel blends. Int. J. Mech. Aerosp. Ind. Mechatron. Manuf. Eng. **2**, 90–96 (2008)
18. Godiganur, S.; Murthy, C.H.S.; Reddy, R.P.: 6BTA 5.9 G2-1 Cummins engine performance and emission tests using methyl ester mahua (*Madhuca indica*) oil/diesel blends. Renew. Energy **34**, 2172–2177 (2009)
19. Sharma, D.; Soni, S.L.; Mathur, J.: Emission reduction in a direct injection diesel engine fueled by neem-diesel blend. Energy Source Part A **31**, 500–508 (2009)
20. Suresh kumar, K.; Velraj, R.; Ganesan, R.: Performance and exhaust emission characteristics of a CI engine fuelled with *Pongamia pinnata* methyl ester (PPME) and its blends with diesel. Renew. Energy **33**, 2294–2302 (2008)
21. Sahoo, P.K.; Das, L.M.; Babu, M.K.G.; Arora, P.; Singh, V.P.; Kumar, N.R. et al.: Comparative evaluation of performance and emission characteristics of jatropha, karanja and polanga based biodiesel as fuel in a tractor engine. Fuel **88**, 1698–1707 (2009)
22. Ganapathy, T.; Gakkhar, R.P.; Murugesan, K.: Optimization of performance parameters of diesel engine with Jatropha biodiesel using response surface methodology. Int. J. Sustain. Energy **30**, S76–S90 (2011)
23. Lapuerta, M.; Herreros, J.M.; Lyons, L.L.; García-Contreras, R.; Brice, Y.: Effect of the alcohol type used in the production of waste cooking oil biodiesel on diesel performance and emissions. Fuel **87**, 3161–3169 (2008)
24. Ahmed, S.; Hassan, M.H.; Abul Kalam, Md.; Ashrafur Rahman, S.M.; Joynul Abedin, Md.; Shahir, A.: An experimental investigation of biodiesel production, characterization, engine performance, emission and noise of *Brassica juncea* methyl ester and its blends. J. Clean. Prod. **79**, 74–81 (2014)
25. Nabi, M.N.; Akhter, M.S.; Shahadat, M.M.Z.: Improvement of engine emissions with conventional diesel fuel and diesel–biodiesel blends. Bioresour. Technol. **97**, 372–378 (2006)
26. Ashrafur Rahman, S.M.; Masjuki, H.H.; Kalam, M.A.; Abedin, M.J.; Sanjid, A.; Sajjad, H.: Production of palm and *Calophyllum inophyllum* based biodiesel and investigation of blend performance and exhaust emission in an unmodified diesel engine at high idling conditions. Energy Convers. Manag. **76**, 362–367 (2013)
27. Antony Miraculas, G.; Bose, N.: Effect of compression ratio on diesel engine performance and emission fueled with tamanu oil methyl ester and its blends. Adv. Mater. Res. **984**, 850–854 (2014)
28. Raheman, H.; Phadatare, A.G.: Diesel engine emissions and performance from blends of karanja methyl ester and diesel. Biomass Bioenergy **27**, 393–397 (2004)
29. Wang, Y.; Zhao, Y.; Xiao, F.; Li, D.: Combustion and emission characteristics of a diesel engine with DME as port premixing fuel under different injection timing. Energy Convers. Manag. **77**, 52–60 (2014)
30. Ashrafur Rahman, S.M.; Masjuki, H.H.; Kalam, M.A.; Abedin, M.J.; Sanjid, A.; Imtenan, S.: Effect of idling on fuel consumption and emissions of a diesel engine fueled by Jatropha biodiesel blends. J. Clean. Prod. **69**, 208–215 (2014)
31. Antony Miraculas, G.; Bose, N.; Edwin Raj, R.: Optimization of process parameters for biodiesel extraction from tamanu oil using design of experiments. J. Renew. Sustain. Energy **6**, 033120 (2014)